

## Helium implanted CuHf as studied by TDPAC and positron lifetime measurements

R GOVINDARAJ, G VENUGOPAL RAO, K P GOPINATHAN\* and B VISWANATHAN  
Materials Science Division, Indira Gandhi Centre for Atomic Research, Kalpakkam 603 102, India  
email: govind@igcar.ernet.in

\*Department of Physics, Cochin University of Science and Technology, Cochin 682 022, India

MS received 21 May 1998; revised 21 November 1998

**Abstract.**  $^{181}\text{Ta}$  time differential perturbed angular correlation (TDPAC) and positron lifetime measurements were carried out on homogeneously  $\alpha$ -implanted CuHf samples. TDPAC measurements indicate the trapping of vacancy clusters and helium associated defect complexes by Hf atoms. The presence of helium-vacancy complexes and helium stabilised voids has been identified by positron lifetime measurements. Further the nucleation and growth stages of helium bubbles have been identified. TDPAC and positron lifetime measurements indicate that Hf atoms act as heterogeneous nucleating centers for helium bubbles. Hf atoms are found to suppress the bubble growth in CuHf as indicated by the results of positron lifetime measurements.

**Keywords.** TDPAC; electric field gradient; Hf solute clusters; positron life-time; helium-bubble.

**PACS Nos** 81.40; 82.20

### 1. Introduction

The problem of helium in metals is of technological importance as helium is produced by  $(n, \alpha)$  reaction in nuclear reactor materials. As helium atoms are insoluble in metals they are strongly attracted by vacancies. Implantation of  $\alpha$  particles in metals leads to the formation of He- $V$  complexes and helium atoms stabilised vacancy clusters [1,2]. In post-irradiation annealing studies, re-arrangement of He- $V$  complexes leading to nucleation and growth of helium bubbles have been reported [3]. As open volume defects bind He atoms strongly, an attractive interaction between the former and impurities present in a sample would lead to formation of He-vacancy cluster complexes as bound to impurities [4]. Therefore depending upon the interaction of an impurity with vacancy there would either be an acceleration [5] or deceleration [6] of nucleation and growth of He bubbles as has been reported in the literature.

The hyperfine interaction of such impurities, meaning the interaction between the nuclear moments of impurities and electromagnetic fields at their sites in a sample [7], provides a powerful method for studying the defects associated with probe nuclei [7,8]. Probe nuclei bound to defects in a cubic and non-magnetic host experience a charge distribution

different from cubic symmetry in most of the cases and hence an electric field gradient. The interaction between the nuclear quadrupole moment of probe nuclei at the isomeric state of interest and the electric field gradient at the sites of the former leads to a perturbation of angular correlation of  $\gamma$  rays emitted in cascade by probe nuclei. The experimental hyperfine interaction parameters enable us to identify the defects that are bound to probe nuclei and their geometry [9–11].

Positron annihilation spectroscopy (PAS) [12,13] is a powerful technique for studying small vacancy clusters. As positron lifetime is sensitive to open volume defects in the sample, it is extensively used in studying the inert gas atoms decorated vacancy clusters. Thus the defect specificity of PAS, combined with the sensitivity to helium decoration, could be effectively used for a quantitative and qualitative understanding of the properties of helium bubbles over a wide range of sizes. There has been a lot of studies on helium in metals by positron annihilation spectroscopic techniques leading to a detailed understanding of nucleation and growth of helium bubbles [13,14]. A comparison of positron lifetime results on helium implanted samples with and without the association of impurities, would enable us to study the influence of impurities in effecting the nucleation and growth of helium bubbles.

Important advantage of combining positron lifetime measurements with the perturbed angular correlation is to identify the open volume defects occurring in the sample either insensitive or non-trapped by TDPAC probe atoms using positron lifetime measurements. For example a cubic cluster of vacancies occurring in a diamagnetic cubic host as trapped by probe atom cannot be detected by TDPAC [8,9]. TDPAC on the other hand could be used to probe all kinds of defects characterised by non-cubic charge distribution that are occurring simultaneously in the sample and trapped by probe atoms. By positron lifetime measurements, it is not possible to distinguish different defects characterised by an almost equivalent average electron density. The resultant hyperfine interaction parameters as obtained by TDPAC measurements depend upon the electron distribution around the probe nuclei. Therefore TDPAC could be used to identify the geometry of defects as bound to probe atoms. A detailed analysis of hyperfine interaction parameters in terms of their variation with annealing treatments and a careful combination with other experimental results for example resistivity, positron lifetime etc, could lead to an unambiguous identification of defects that are trapped by probe atoms [11].

In dilute alloy systems the binding of defects by more than one solute atom is important to be considered if solute atom clustering is observed in the reference sample before subjecting it to any defect treatments. This is mainly due to a high stability of the resultant defect configuration due to more than one solute atom trapping the defects concerned. Perturbed angular correlation measurements conducted on quenched  $\underline{AlIn}$  alloys showed the appearance of defect complexes containing more than one In atom at temperatures above 250 K [14,15]. In the quenched  $\underline{AlIn}$  sample, the clustering of In atoms has been observed by  $^{111}\text{Cd}$  TDPAC measurements [16,17]. Positron annihilation spectroscopy has been used extensively to study the precipitation in metals [18,19]. The effect of the decoration of vacancy by more than one solute atom has been reported in quenched  $\underline{CuIn}$  alloys by Doppler broadening measurements of the positron annihilated 511 keV  $\gamma$  ray [18].

The present experiment aims at the following. (1) To study the defects occurring in a homogeneously helium implanted  $\underline{CuHf}$ , and the evolution of these defects with isochronal annealing treatments of the sample by TDPAC and positron lifetime measurements. This involves studying the defects that are trapped by Hf atoms and the evolution of these with

isochronal annealing treatments by perturbed angular correlation measurements. (2) To verify independently the presence of open volume defects and their decoration by He atoms by positron lifetime measurements. (3) To study the binding of helium implantation induced defects by Hf impurities based on comparison of positron lifetime results obtained by measurements carried out on samples with and without Hf impurities, subjected to identical helium implantations. (4) To study the nucleation and growth stages of helium bubbles and also to compute the bubble parameters such as bubble concentration and radii based on the results of positron lifetime measurements conducted following different annealing treatments.

## 2. Experimental details

Cu with 1 wt% Hf, each of 99.8% purity, were arc melted in a helium atmosphere and homogenised by prolonged annealing to prepare CuHf samples of dimension 10 mm × 2 mm × 245 μm and 10 mm × 10mm × 245 μm for TDPAC and positron lifetime measurements respectively. These samples were subsequently annealed at 1273 K at a pressure of 10<sup>-6</sup> torr for 3 hours to obtain defect free reference samples. These samples were homogeneously implanted with α particles of 40 MeV energy from a cyclotron to a dose of 100 ppm. The temperature of the sample during irradiation was 313 ± 5 K. Subsequently the samples meant for TDPAC measurements were thermal neutron irradiated at the CIRUS reactor at Bhabha Atomic Research Centre, Bombay, to a fluence of 2 × 10<sup>22</sup> n/m<sup>2</sup>, to produce <sup>181</sup>Ta probe nuclei in the samples by the reaction <sup>180</sup>Hf (n, γ) <sup>181</sup>Hf → β<sup>-</sup> <sup>181</sup>Ta.

The TDPAC of the 133–482 keV γ – γ cascade of <sup>181</sup>Ta was measured by a three detector twin fast-slow coincidence setup having NaI(Tl) detectors. One of the detectors was gated for the START (133 keV) γ-ray, with respect to which the other two detectors were fixed at 90° and 180° for the detection of the STOP (482 keV) γ-ray. The time delayed coincidence spectra were obtained in the form of count rate as a function of the time elapsed after the emission of first γ-ray. The two time spectra W(90°, t) and W(180°, t) were recorded simultaneously. The prompt time resolution of the setup measured with a <sup>60</sup>Co source was 2.2 ns FWHM when gated for the above cascade of <sup>181</sup>Ta [20]. From the delayed coincidence spectra W(90°, t) and W(180°, t), the normalised anisotropy function R(t) was calculated as

$$R(t) = A_2 G_2(t) = 2 \times \frac{[W(180^\circ, t) - W(90^\circ, t)]}{[W(180^\circ, t) + 2W(90^\circ, t)]}, \quad (1)$$

where A<sub>2</sub> is effective anisotropy coefficient and G<sub>2</sub>(t) is the perturbation factor. W(90°, t) and W(180°, t) are the coincidence count rates at 90° and 180° respectively between the START and STOP detectors.

The 133–482 keV γ – γ cascade of the probe nucleus <sup>181</sup>Ta is separated by an intermediate state. The spin of this isomeric state is 5/2. The spin degeneracy of the intermediate state of the nucleus is partially removed due to the interaction between the quadrupole moment of the nucleus at this state and EFG at its site. The transition between these substrates due to the above quadrupole interaction results in the appearance of three frequencies which are the splittings between the doubly-degenerate ±5/2, ±3/2 and ±1/2 hyperfine levels.

Therefore the R(t) spectra were least squares fitted to the function [8],

$$R(t) = A_2 \sum_{i=0}^n f_i G_2^i(t), \quad (2)$$

where

$$G_2^i(t) = \sum_{m=0}^3 a_m^i \exp[-\delta_i k_m^i(\eta_i) \omega_{Qi} t] \cos[k_m^i(\eta_i) \omega_{Qi} t], \quad (3)$$

where  $n$  occurring in (2) is the number of frequency components that are fitted to the anisotropy function  $R(t)$ . This has been based on the fourier transformed spectra of  $R(t)$  and the value of the normalised degree of freedom obtained during the fitting of the  $R(t)$  spectra to the above equation. The value of  $G_2^0(t)=1$ .

Also  $k_0 = 0$ ,  $k_1(\eta_i) + k_2(\eta_i) = k_3(\eta_i)$  and  $\sum_{m=0}^3 a_m^i(\eta_i) = 1$ .

The spin value of the isomeric state of  $^{181}\text{Ta}$  being  $I = 5/2$  we have

$$\langle \nu_{Qi} \rangle = eQV_{zz}^i/h = 10\omega_{Qi}/3\pi, \quad (4)$$

where  $V_{zz}^i$  is the principal component of the electric field gradient (EFG) tensor. When the EFG is not axially symmetric, the asymmetry parameter  $\eta_i = (V_{xx}^i - V_{yy}^i)/V_{zz}^i$  where  $|V_{zz}^i| \geq |V_{yy}^i| \geq |V_{xx}^i|$  is extracted from the fit of  $R(t)$  data to (2). The values of  $k_m^i$  depend on  $\eta_i$ .

The experimental detail of positron lifetime measurements is briefly described as follows. Radionuclide  $^{22}\text{Na}$  coated thin nickel foil, sandwiched between two identical samples of interest, forms the source of positrons. Positrons predominantly annihilate with electrons in metals by two photon annihilation mode with the emission of two 511 keV  $\gamma$  rays at nearly  $180^\circ$  [12]. Emission of positron from  $^{22}\text{Na}$  by  $\beta$  decay is accompanied by a 1280 keV  $\gamma$  ray. The lifetime of positron in a medium is measured as the time elapsed between the emission of 1280 and 511 keV  $\gamma$  rays. Positron lifetime measurements have been carried out on the sample using a fast-fast coincidence spectrometer having plastic scintillator detectors with a time resolution of 220 ps (FWHM). The exponential decay spectrum of positrons injected into the sample from the radionuclide  $^{22}\text{Na}$  by beta decay can be decomposed to give the fractions that annihilate with particular lifetimes  $\tau_i$ . In the present case the exponential decay spectrum has been fitted with the following expression based on the two component fitting analysis [12].

$$I(t) = I_1 \exp(-t/\tau_1) + I_2 \exp(-t/\tau_2), \quad (5)$$

where  $\tau_1, \tau_2$  are the characteristic lifetimes and  $I_1$  and  $I_2$  the corresponding intensities.

Time differential perturbed angular correlation and positron lifetime measurements were done on the respective helium implanted samples at room temperature following each step of an isochronal annealing treatment from 323 to 1273 K in steps of 50 K and a step duration of 30 minutes.

### 3. Results and discussion

The reference  $\underline{\text{Cu}}\text{Hf}$  sample is characterised by TDPAC and EDAX measurements. The data analysed time dependent anisotropy spectrum  $R(t)$  and its Fourier transform for  $^{181}\text{Ta}$

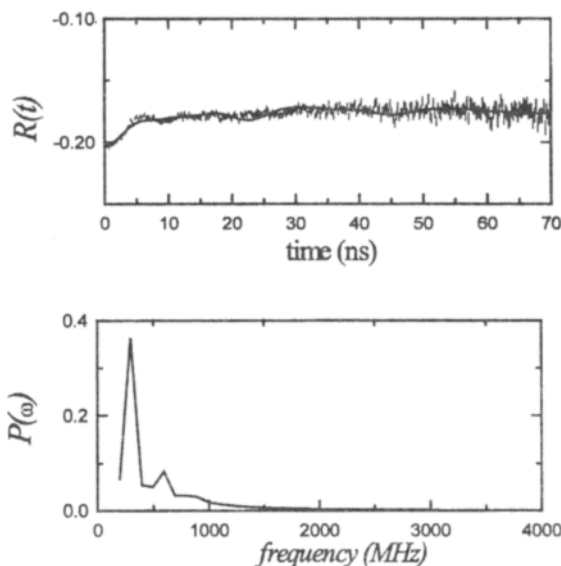


**Figure 1.** TDPAC spectrum  $R(t)$  and its Fourier transform  $P(\omega)$  in the reference  $\underline{\text{CuHf}}$ .

in the reference  $\underline{\text{CuHf}}$  sample is shown in figure 1. The  $R(t)$  spectrum shows the presence of a single periodic component, while the Fourier spectrum  $P(\omega)$  shows the peaks at the fundamental and almost close to second and third harmonic components of the quadrupole frequency with the fundamental component lying at 290 MHz. The data analysis of the  $R(t)$  spectrum indicates that a fraction  $0.1 \pm 0.01$  probe atoms experiences a quadrupole frequency of  $290 \pm 5$  MHz with an asymmetry parameter  $0.08 \pm 0.04$  and a damping parameter  $0.08 \pm 0.03$ . The remaining fraction of probe nuclei experiences a zero quadrupole frequency implying that these are substitutional and defect free in  $fcc$  Cu matrix. The observed defect component indicated by a quadrupole frequency of  $290 \pm 5$  MHz is attributed to the probe atoms associated with Hf solute clusters, as the quadrupole parameters are almost the same as that experienced by  $^{181}\text{Ta}$  probe atoms in  $hcp$  Hf matrix [21]. The presence of Hf rich zones in the sample is further evidenced by EDAX (energy dispersive x-ray analysis) measurements. The EDAX spectrum confirming the presence of Hf rich zones are shown in figure 2.

Positron decay spectra in helium implanted  $\underline{\text{CuHf}}$  for a few isochronal annealing treatments of the sample viz 323, 823 and 1023 K are shown in figure 3. The analysis of the positron decay spectrum based on a two-component fit indicates the following resolved lifetime parameters in the as-implanted state viz.,  $\tau_1 = 200 \pm$  ps,  $\tau_2 = 480 \pm 40$  ps and  $I_1 = 0.95 \pm 0.02$ . From figure 4, which shows the variation of the resolved lifetime parameters with isochronal annealing temperature it is observed that the values of  $\tau_1$  and  $\tau_2$  decrease with annealing temperature and reach a minimum at around 800 K.  $I_2$  remains constant at 0.05 during the annealing interval between 300 and 600 K. Beyond 600 K,  $I_2$  increases and reaches a maximum value of 0.4 at 800 K. The value of  $\tau_1$  remains almost constant at  $115 \pm 5$  ps for annealing treatments beyond 800 K. In the annealing interval

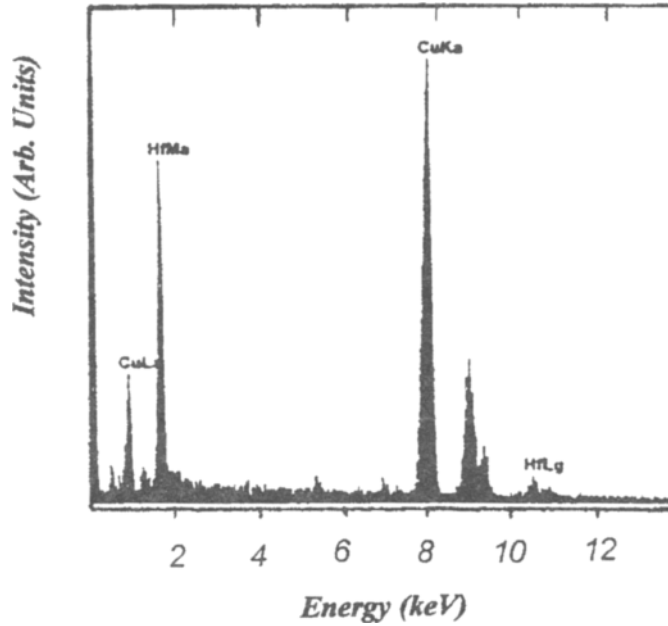


**Figure 2.** Energy dispersive x-ray analysis (EDAX) spectra showing the presence of Hf rich zones in  $\underline{\text{CuHf}}$ .

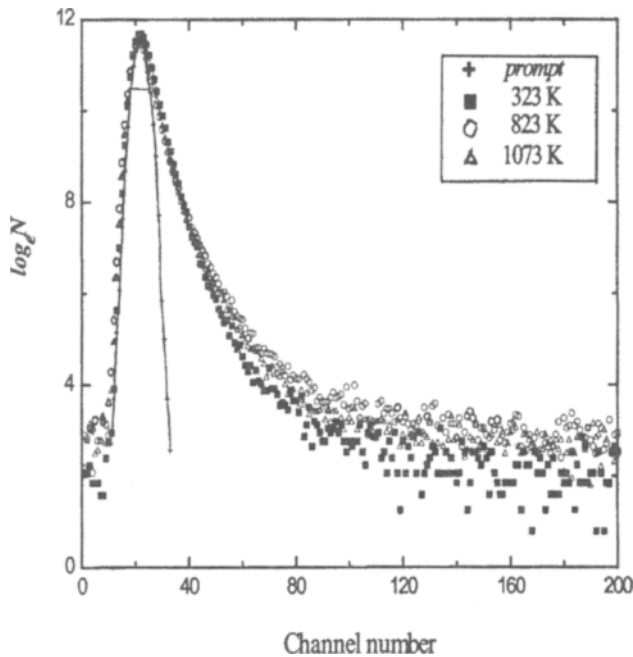


**Figure 3.** The positron decay spectra at room temperature in helium implanted  $\underline{5\text{CuHf}}$  sample subjected to annealing treatments at 323, 823 and 1073 K. Also shown in the figure is the prompt spectrum obtained with  $^{60}\text{Co}$  having a FWHM of 220 ps.

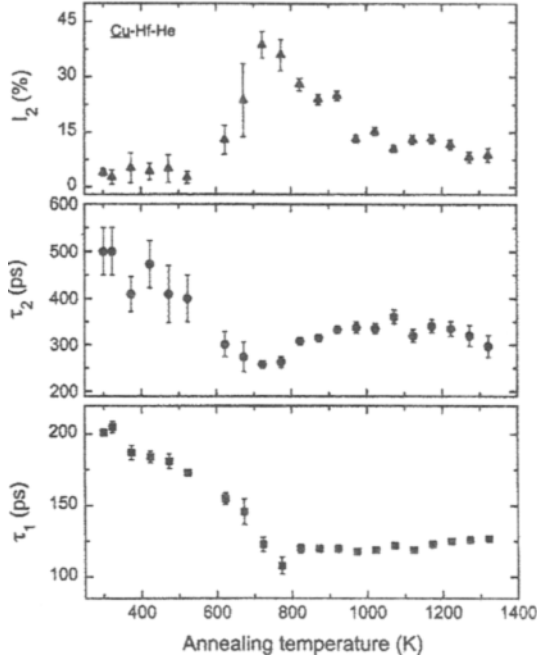


**Figure 4.** Variation of the resolved positron lifetime parameters viz.  $\tau_1$ ,  $\tau_2$  and  $I_2$  with isochronal annealing temperature.

800–1100 K,  $\tau_2$  increases towards saturation at a value of  $340 \pm 4$  ps. Between 1100 and 1373 K,  $\tau_2$  decreases to a value of  $280 \pm 3$  ps and  $I_2$  remains nearly constant. The above results are in accordance with figure 3 showing the positron decay spectra in helium implanted CuHf following the isochronal annealing treatments of the sample at 323, 823 and 1023 K respectively.

The dominant fraction  $I_1$  corresponding to the lifetime  $\tau_1$  in the as implanted CuHf sample is identified to be due to positron trapping at He-V complexes in the sample. In the process of homogeneous helium implantation a large number of vacancies is produced. The TRIM (transmission of ion in matter) code [22] is used to find out the concentration of vacancies produced due to the homogeneous helium implantation based on the attenuation of 40 MeV alpha beam by aluminium foils of different thicknesses used in the irradiation. The concentration of vacancy is computed to be around  $1.56 \times 10^{27} \text{ m}^{-3}$  without taking into account vacancy loss to sinks. As there is a large overlap of the vacancy and helium profiles as observed by TRIM code, there is an appreciable probability for the formation of helium-vacancy complexes, as vacancies are strong trapping centers for helium atoms. The lifetime component characterised by  $\tau_1$  also include the He-V complexes trapped by Hf impurities. This is based on the observation that the value of  $\tau_1$  (200 ps) is slightly higher than that in the as-implanted pure Cu sample (175 ps) indicating that in the CuHf sample,  $\tau_1$  includes contributions from both Hf associated He-V complexes and Hf-free He-V complexes. Also, the lifetime of positron in a defect free and at a monovacancy in Cu matrix are 110 ps and 175 ps respectively [23]. The lifetime of the positrons annihilating at vacancy clusters containing two and three vacancies has been computed to be around

240, 310 ps respectively by Jena *et al* [24]. Therefore, the fraction  $I_2$  corresponding to the lifetime value  $\tau_2 = 480$  ps is interpreted to be due to the annihilation of positrons at large vacancy clusters. The fraction  $I_2$  might very well include the isolated vacancy clusters in addition to vacancy clusters trapped by Hf impurities.

The decrease in  $\tau_1$  with the isochronal annealing treatment is due to the dissociation of He-V complexes as trapped by Hf impurities. The dissociated helium atoms decorate the isolated vacancy clusters and vacancy clusters bound to Hf impurities represented by the lifetime parameter  $\tau_2$ . This results in decrease in the value of  $\tau_2$ . This is accompanied by an increase in  $I_2$  at the cost of  $I_1$ , due to the above reason. The minimum in  $\tau_2$  and  $\tau_1$  are observed to occur at the same temperature of 775 K. This implies that the onset of the nucleation of helium bubbles in CuHf occurs at this temperature [25]. The supply of helium and vacancies available from the dissociating He-V complexes aids bubble nucleation in CuHf at a higher annealing temperature of 775 K. Annealing treatment between 775 and 1000 K (figure 4) shows a constant behaviour of  $\tau_1$  at 116 ps. This is identified as due to bulk annihilations at defect free sites in a Cu matrix. The value of  $\tau_2$  increases accompanied by a decrease in  $I_2$ . This is due to bubble growth involving size relaxation at the cost of bubble density. This means that overpressurised helium bubbles of small radii coalesce to form bubbles of larger radii with reduced pressure, leading to a decrease in the number density of the bubbles [3]. This reduction in number density of helium bubbles leads to a decrease in  $I_2$  beyond 775 K. On comparison of the results of positron lifetime measurements in pure Cu subjected to an identical helium implantation [24] it can be observed that the onset temperature of the nucleation of helium bubbles in CuHf is higher than that in pure Cu.

The time dependent anisotropy spectra,  $R(t)$  obtained in the as-implanted and in the sample following isochronal annealing measurements were non-linear least square fitted with three components using (2) to obtain optimal values of variance of the fit. The fitted anisotropy spectra of helium implanted CuHf sample for a few isochronal annealing temperatures are shown in figure 5.

Data analysis of the  $R(t)$  spectra as fitted with the above expression in the helium implanted sample has revealed the presence of the following hyperfine interaction parameters viz.,  $\nu_{Q1}=225 \pm 5$  MHz,  $f_1=0.14 \pm 0.02$ ,  $\delta_1=0.6 \pm 0.06$ ,  $\eta_1=0.33 \pm 0.11$ ,  $\nu_{Q2}= 755 \pm 20$  MHz,  $f_2=0.1 \pm 0.02$ ,  $\delta_2=0.2 \pm 0.04$  and  $\eta_2=0.35 \pm 0.05$ . As unique hyperfine interaction parameters are observed in the measurement, these can be associated with defects of well defined geometry. The variation of hyperfine interaction parameters with annealing temperature are shown in figures 6 and 7.

It can be seen from the figure 6 that  $\nu_{Q1}$  increases steadily with increasing annealing temperature and attains a value of  $289 \pm 5$  MHz. The value of  $f_1$  reaches a maximum of  $0.2 \pm 0.03$  following the annealing treatment at 373 K and thereafter remains constant at  $0.14 \pm 0.02$ . The value of  $\delta_1$  decreases steadily beyond 573 K and reaches a value of  $0.35 \pm 0.06$  at 773 K. The value of  $\eta_1$  is seen to show a steady increase in the measured annealing range. From figure 7 three temperature regions can be discerned: Isochronal annealing treatments below 475 K leads to a steady decrease in  $\nu_{Q2}$  accompanied by a decrease in  $\eta_2$ . The value of  $f_2$  and  $\delta_2$  are seen to increase in this temperature regime. Annealing treatments in the interval between 475 and 775 K results in a constant value of  $\nu_{Q2}$  at  $620 \pm 5$  MHz and  $\eta_2$  at  $0.1 \pm 0.04$ . The value of  $f_2$  shows a steady decrease from  $0.17 \pm 0.05$  to  $0.12 \pm 0.04$ , while the value of  $\delta_2$  attains a maximum around 575 K. Annealing beyond 775 K is marked by a sharp increase in  $\nu_{Q2}$  and  $\eta_2$  whereas  $f_2$  and  $\delta_2$

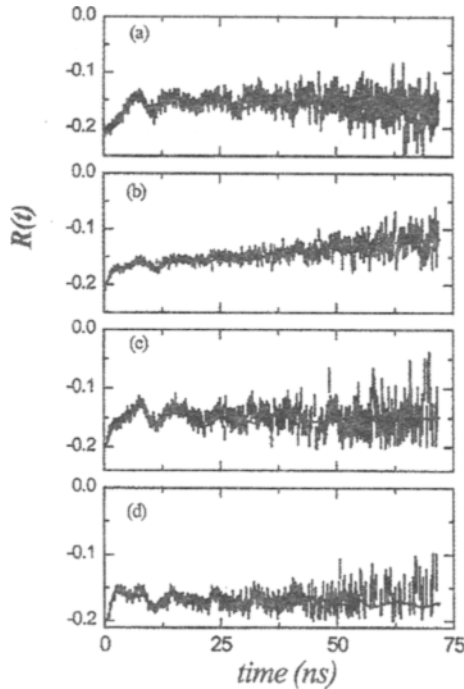


**Figure 5.** The TDPAC spectra in the room temperature helium ions implanted  $\underline{\text{CuHf}}$  sample subjected to following annealing treatments. (a) as implanted (b)  $T_a = 473$  K (c)  $T_a = 773$  K and (d)  $T_a = 873$  K.

show a steady decrease.

The fraction  $f_0$  is due to probe atoms occupying cubic charge environment experiencing a zero EFG. In general this fraction is completely contributed by probe atoms occupying defect free substitutional sites in  $fcc$ . In the helium implanted sample probe atoms occupying the substitutional sites in the sample associated with tetrahedron of vacancies might also contribute for  $f_0$  in addition to the probe atoms occupying defect free, substitutional sites in  $fcc$ . The presence of vacancy clusters in the helium implanted sample is evidenced by positron lifetime measurements ( $\tau_2 = 480 \pm 40$  ps) as shown in figure 4.

In the following, the two defects associated hyperfine interaction parameters are identified based on their magnitudes, their temperature variation, in conjunction with the positron lifetime results.

The defect associated fraction of the probe atoms as observed in the reference  $\underline{\text{CuHf}}$  sample (*i.e.*, the component characterised by a quadrupole frequency of  $290 \pm 5$  MHz) was not present in the as implanted sample. The quadrupole frequency  $\nu_{Q1}$  and the asymmetry parameter  $\eta_1$  corresponding to the fraction  $f_1$  of the probe atoms are  $\nu_{Q1} = 225 \pm 5$  MHz and  $\eta_1 = 0.33 \pm 0.11$  and these are different from the hyperfine interaction parameters as observed in the reference sample.

First it can be observed that the fraction  $f_1$  of probe atoms is characterised by a non-zero

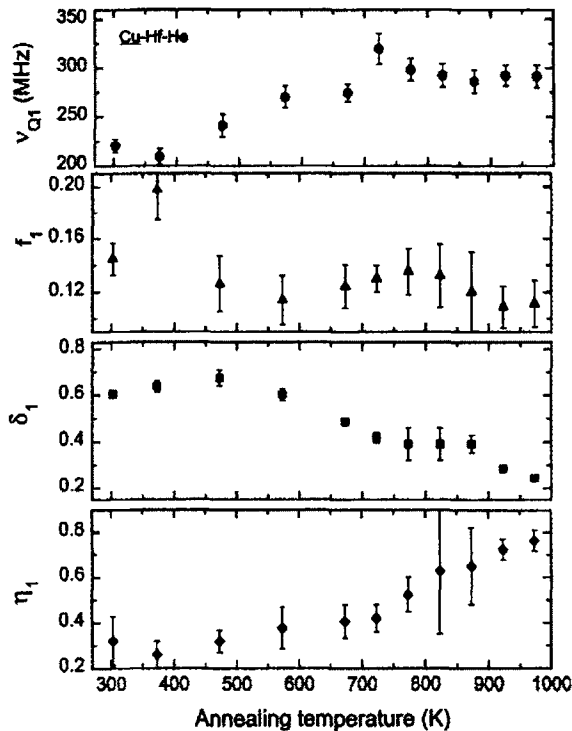


**Figure 6.** Variation of hyperfine interaction parameters viz.  $\nu_{Q1}$ ,  $f_1$ ,  $\eta_1$  and  $\delta_1$  with isochronal annealing temperature.

asymmetry parameter. This rules out the concerned defect to be a monovacancy (axially symmetric along  $\langle 110 \rangle$ ) or a di-vacancy (axially symmetric along  $\langle 100 \rangle$ ,  $\langle 110 \rangle$ ) as these are characterised by a zero asymmetry parameter [10]. Further, the fraction  $f_1$  cannot be due to Hf solute atoms trapping He associated vacancies. This is due to the reasoning that the present experiment involves un-correlated damage studies [26]. If the fraction  $f_1$  were to be associated with helium associated vacancies then the value of the order of 0.14 is unlikely for the concentration of helium/Hf involved.

The value of the quadrupole frequency  $\nu_{Q1}$  ( $225 \pm 4$  MHz) in the as implanted sample lies below the quadrupole frequency as experienced by the probe atoms associated with Hf solute clusters in the reference sample. Isochronal annealing treatment of the sample leads to a steady increase in  $\nu_{Q1}$  towards the quadrupole frequency of probe atoms in Hf matrix (*i.e.*,  $290 \pm 5$  MHz). Based on the observation of the variation of the quadrupole frequency  $\nu_{Q1}$  with isochronal annealing temperature and the magnitude of the fraction of probe atoms associated with the defect concerned, the fraction  $f_1$  is interpreted to be due to probe atoms associated with Hf solute atom clusters trapping vacancies. The trapping of vacancies by more than one Hf atom is quite likely to be the case because of the presence of Hf solute clusters in the reference sample. The helium decorated defect complexes are more stable than the undecorated defect complex [27]. If the probe-vacancies complexes

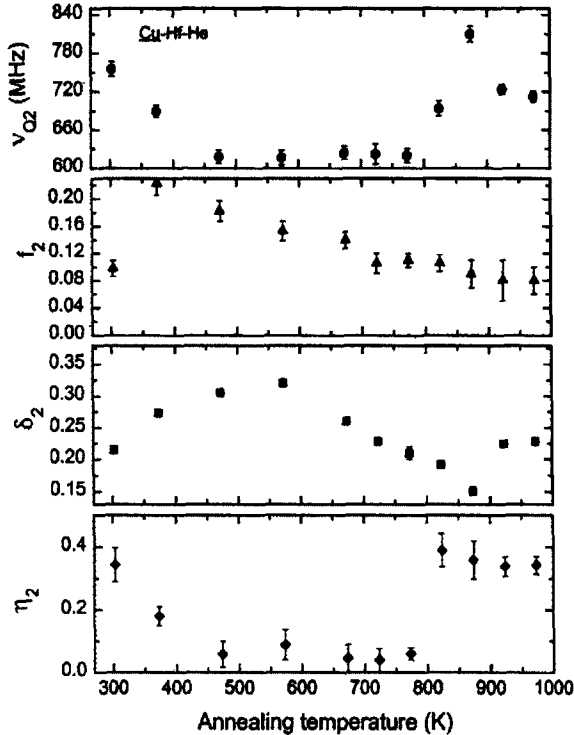


Figure 7. Variation of hyperfine interaction parameters viz.  $\nu_{Q2}$ ,  $f_2$ ,  $\eta_2$  and  $\delta_2$  with isochronal annealing temperature.

were to be associated with helium atoms, it would have resulted in highly stable defect complexes which might prevent the formation of hafnium solute clusters.

The steady increase in the quadrupole frequency as experienced by the fraction  $f_1$  of the probe atoms with annealing treatment of the sample is understood to be due to the evaporation of vacancies as trapped by Hf atom clusters. It is noticed that in this temperature range positron lifetime component  $\tau_1$  (figure 4) associated with vacancy type defects is seen to decrease.

In trying to understand the defects, associated with the fraction  $f_2$  of probe atoms responsible for the variation of hyperfine interaction parameters with annealing temperature as shown in figure 7, the results of positron lifetime measurements are referred. The annealing stage below 475 K indicates the presence of vacancy clusters as deduced from positron lifetime measurements shown in figure 4. Hf atoms associated with solute clusters trapping small vacancy clusters can lead to a large  $\nu_{Q2}$ . The decoration of the vacancy clusters with helium atoms, due to the dissociation of He-V complexes between 475 and 775 K, is shown as a decrease in  $\tau_2$ . The annealing stage between 475 and 775 K is marked by a constant value of  $\nu_{Q2}$  and  $\eta_2$  as shown in figure 7. This can be attributed to He stabilised vacancy clusters associated with Hf impurities. The annealing stage beyond 800 K which corresponds to the growth of helium bubble is marked by an increase of  $\nu_{Q2}$  and  $\eta_2$ . This stage corresponds to bubble growth as seen from the results of positron lifetime measurements.

#### 4. Extraction of helium bubble parameters from positron lifetime results

The helium bubble parameters such as helium atom density ( $n_{\text{He}}$ ) inside the bubble, bubble radius ( $R_b$ ) and bubble concentration ( $C_b$ ) have been determined from an analysis of experimental positron lifetime results based on the procedure reported earlier [3]. Based on the positron surface state model [28], the most stable positron state is at the surface of the bubble of radii  $> 5\text{\AA}$ . Considering the gas-metal interface, positrons will be annihilating with electrons associated with both the metal and helium. As these two annihilation processes are independent the total annihilation rate can be written as

$$\lambda_{\text{bubble}} = \lambda_{\text{He}} + \lambda_{\text{metal}}. \quad (6)$$

$\lambda_{\text{metal}}$  is characteristic of the annihilation rate for clean metal surface. This is almost same for most of the metals having a value of  $\approx 2 \text{ ns}^{-1}$ .  $\lambda_{\text{He}}$  depends on the helium atom density  $n_{\text{He}}$ . The relationship connecting bubble lifetime  $\tau_2$  and helium atom density  $n_{\text{He}}$  is given by [28]

$$\tau_2 = 500 - 23.5n_{\text{He}}(10^{28}\text{m}^{-3}). \quad (7)$$

Although the above equation was originally proposed for Al-He system it can be applied as a first approximation for most metal-He systems [28,29]. Using  $\tau_2$  in the above equation,  $n_{\text{He}}$  can be determined. On the basis of two state trapping model [29], the trapping rate,  $K_b$ , into the bubbles can be deduced from the measured lifetime parameters as

$$K_b = I_2(\lambda_1 - \lambda_2), \quad (8)$$

where  $\lambda_1$  and  $\lambda_2$  are experimental annihilation rates in the bulk and bubble respectively and  $I_2$  is the intensity of the bubble lifetime component. The trapping rate  $K_b$  can be related to bubble concentration,  $C_b$ , as

$$K_b = \mu_b C_b, \quad (9)$$

where  $\mu_b$  is the specific trapping rate of positrons to the bubble. The size dependence of  $\mu_b$  is taken into account by using a semi-empirical relation for  $\mu_b$ , given by [28]

$$\mu_b = \left[ \frac{1}{AR_b} + \frac{1}{BR_b^2} \right]^{-1}, \quad (10)$$

where the constants are given by  $A = 9.07 \times 10^{16} \text{ nm}^{-1} \text{ s}^{-1}$  and  $B = 3.3 \times 10^{16} \text{ nm}^{-2} \text{ s}^{-1}$ . If the total gas concentration,  $C_{\text{He}}$ , implanted into the sample is known and all the gas is assumed to be contained in spherical bubbles, then the helium inventory equation can be written as

$$C_{\text{He}} = \frac{4\pi R_b^3 n_{\text{He}} C_b}{3}. \quad (11)$$

The above assumption that all the input helium is contained in the bubbles is justified because of the fact that samples of thickness greater than  $100 \mu\text{m}$  are used for PAS and helium loss from the bubble to the sample surface is expected to be negligible.

Using the equations (7), (8), (9), (10) and (11), an equation for  $R_b$  can be written as

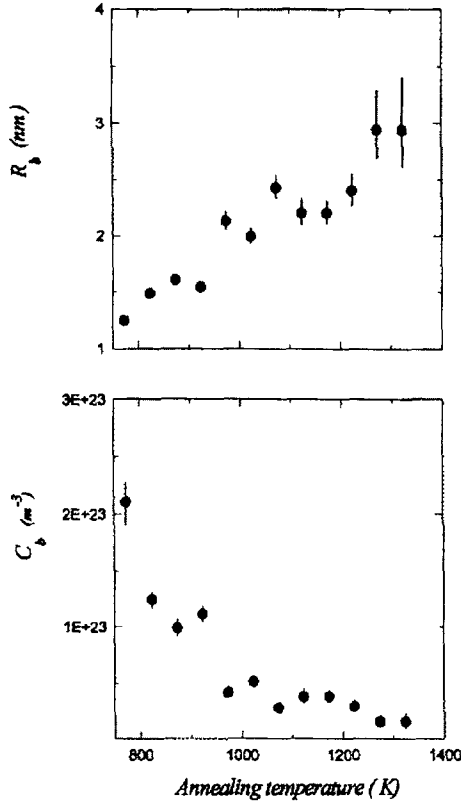


Figure 8. Variation of (a) bubble radius and (b) bubble concentration with annealing temperature in the helium implanted CuHf as deduced from the positron lifetime results.

$$BR_b^2 + AR_b - 3AB \left( \frac{C_{He}}{4\pi I_2(\lambda_1 - \lambda_2)n_{He}} \right) = 0. \quad (12)$$

With  $n_{He}$  known from (6) and with the known value of  $C_{He}$ , the above equation is solved for  $R_b$ . Once  $R_b$  is known, the bubble concentration  $C_b$  can be obtained using (10).

The variation of  $R_b$  and  $C_b$ , as deduced from the above discussed analysis scheme are shown in figure 8a and 8b.  $R_b$  increases from a value of 13Å around 800 K to 30Å at around 1300 K, while  $C_b$  decreases from  $2 \times 10^{23}$  to  $9 \times 10^{22} m^{-3}$  in the same annealing interval. This establishes quantitatively the helium bubble growth. Based on the results of positron lifetime measurements carried out on pure Cu sample subjected to identical helium implantation [6] Amarendra *et al* have reported that the value of average bubble radius  $R_b$  increases roughly from 12 Å around 700 K to 36 Å around 1175 K. In the same annealing interval  $C_b$  is reported to decrease from  $10^{22}$  to  $6.4 \times 10^{20} m^{-3}$ . On comparison of the results in pure Cu and CuHf it is understandable that the binding of He-V complexes by Hf atoms in the latter has essentially led to the presence of a larger concentration of smaller helium bubbles in the same annealing interval. This implies that Hf atoms in CuHf suppress the helium bubble growth.

## 5. Conclusions

In the reference  $\underline{\text{CuHf}}$  sample, the presence of Hf atom solute clusters has been observed by TDPAC measurements and evidenced by EDAX measurements. TDPAC measurements in helium implanted  $\underline{\text{CuHf}}$  indicate the trapping of vacancies by Hf clusters for annealing intervals below 475 K. Positron lifetime measurements indicate the formation of He-V-Hf complexes. These further indicate the migration of He atoms in the sample around 500 K. The TDPAC measurements show the trapping of helium atoms by the vacancies associated with the Hf solute atom clusters leading to the formation of a stable defect complex for annealing treatments above 500 K. In the same temperature interval, positron lifetime measurements indicate the decoration of vacancy clusters by helium atoms leading to the formation of bubble nuclei. The on-set temperature of nucleation of helium bubble in  $\underline{\text{CuHf}}$  is seen to be higher than that of pure Cu. Bubble growth is reflected by a sharp increase in  $\nu_{Q2}$  and  $\eta_2$  around 800 K. This correlates with the increase in positron lifetime  $\tau_2$ . Comparison of the computed results of bubble parameters with annealing temperature on pure Cu and  $\underline{\text{CuHf}}$  indicate that Hf atoms in  $\underline{\text{CuHf}}$  suppress the helium bubble growth.

## Acknowledgements

We thank R Rajaraman for helping in the irradiation experiments. We thank C S Sundar and G Amarendra for useful discussions. Our sincere thanks are due to Vijayalakshmi, Saroja Saibaba and G Mythili for EDAX measurements.

## References

- [1] H Ullmaier, *Rad. Eff.* **78**, 1 (1983)
- [2] W D Wilson, C L Bisson and M I Bakes, *Phys. Rev.* **B24**, 5616 (1981)
- [3] G Amarendra, B Viswanathan, A Bharathi and K P Gopinathan, *Phys. Rev.* **B45**, 10231 (1992)
- [4] F Plieter, K Post, M Mohsen and T S Wierenga, *Phys. Lett.* **A101**, 363 (1984)
- [5] C D Van Siclen and R N Wright, *Phys. Rev. Lett.* **26**, 3892 (1992)
- [6] G Amarendra, B Viswanathan, R Rajaraman, S Srinivasan and K P Gopinathan, *Philos. Mag. Lett.* **65**, 77 (1992)
- [7] E Recknagel, G Schatz and Th Wichert, in *Hyperfine interactions of radioactive nuclei*, Edited by J Christiansen (Springer-Verlag, Heidelberg, 1983)
- [8] H Rinneberg, W Semmler and G Antsberger, *Phys. Lett.* **A64**, 57 (1978)
- [9] L Niesen, *Hyp. Int.* **10**, 619 (1981)
- [10] Gary Collins S, Shropshire L Steven and Fan Jiawen, *Hyp. Int.* **62**, 1 (1990)
- [11] Th Wichert, *Rad. Eff.* **78**, 177 (1993)
- [12] *Positron solid state physics*, Edited by W Brandt and A Dupasquier (North-Holland, Amsterdam, 1983)
- [13] *Positron annihilation studies in materials science*, Edited by B Viswanathan and C S Sundar, *Metals, Materials and Processes*, 1 (1996)
- [14] M L Swanson, L M Howe, A F Qunneville, Th Wichert and M Deicher, *J. Phys.* **78**, 1603 (1984)
- [15] M L Swanson, Th Wichert, L M Howe and A F Qunneville, *Nucl. Instrum. Methods* **B15**, 413 (1986)

- [16] J A Jackman, Th Wichert and M L Swanson, *J. Phys.* **78**, 1357 (1987)
- [17] G J Kemerlink and F Pleiter, *Script. Met.* **19**, 881 (1985)
- [18] W Luhr Tanck, M Ederhof, A Sager and H Bosse, *Mater. Sci. Forum.* **15-18**, 629 (1987)
- [19] A Bharathi, C S Sundar and K P Gopinathan, *Philos. Mag.* **A58**, 705 (1988)
- [20] R Govindaraj and K P Gopinathan, *J. Nucl. Mater.* **231**, 141 (1996)
- [21] R Vianden, *Hyp. Int.* **15-16**, 1081 (1983)
- [22] J P Biersack and L G Haggmark, *Nucl. Instrum. Methods* **174**, 257 (1980)
- [23] T Gorecki, *Mater. Sci. Forum.* **105-110**, 643 (1992)
- [24] P Jena and B K Rao, *Phys. Rev.* **B31**, 5634 (1985)
- [25] G Amarendra, B Viswanathan and K P Gopinathan, *Radiation effects and defects in solids.* **118**, 357 (1991)
- [26] F Pleiter, W Z Venema and A R Arends, *Hyp. Int.* **4**, 693 (1978)
- [27] S E Donnelly, *Rad. Eff.* **78**, 1 (1983)
- [28] K O Jensen and R M Nieminen, *Phys. Rev.* **B35**, 2087 (1987)
- [29] K O Jensen and R M Nieminen, *Phys. Rev.* **B36**, 8219 (1987)